

Physics with prompt photons at SPD

Alexey Guskov on behalf of the SPD working group

Dzhelepov Laboratory of Nuclear Problems, Joint Institute for Nuclear Research, Joliot-Curie 6, Dubna Russia

E-mail: avg@jinr.ru

Abstract. Prompt photons is a proven instrument for exploration of the gluonic structure of hadrons. The SPD experiment at the NICA collider plans to use prompt photons for study of the gluon contribution to the spin structure of the nucleon in the polarised proton-proton and deuteron-deuteron collisions.

1. Introduction

NICA (Nuclotron-based Ion Collider fAility) is a new accelerator complex designed at the Joint Institute for Nuclear Research (Dubna, Russia) to study properties of baryonic matter. In the first interaction point of the new collider the MultiPurpose Detector (MPD) intends to study properties of hot dense nuclear matter in heavy ions collisions. The Spin Physics Detector (SPD) in the second interaction point will be constructed for investigation of the nucleon spin structure in collisions of longitudinally and transversely polarised protons and deuterons at \sqrt{s} up to 27 GeV and luminosity up to $10^{32} s^{-1}cm^{-2}$. The measurement of TMD PDFs for quarks and gluons using such reactions as the Drell-Yan process, charmonia and prompt photon production is the main goal of the experiment [1, 2].

Prompt-photon production is a proven instrument for exploration of the gluonic structure of hadrons. Unpolarised and polarised physics with prompt photons and experimental conditions of their registration in the SPD setup will be discussed below.

2. Prompt photons at low energies

Prompt photons are photons produced in the hard scattering of partons. According to the factorization theorem, the inclusive cross section for the production of a prompt photon in a collision of hadrons h_A and h_B can be written as follows:

$$d\sigma_{AB\rightarrow\gamma X} = \sum_{a,b=q,\bar{q},g} \int dx_a dx_b f_a^A(x_a, Q^2) f_b^B(x_b, \mu^2) d\sigma_{ab\rightarrow\gamma x}(x_a, x_b, Q^2). \quad (1)$$

The function f_a^A (f_b^B) is the parton density for hadron h_A (h_B), x_a (x_b) is the fraction of the momentum of hadron h_A (h_B) carried by parton a (b) and Q^2 is the square of the 4-momentum transferred in the hard scattering process, and $\sigma_{ab\rightarrow\gamma x}(x_a, x_b, Q^2)$ represents the cross section for the hard scattering of partons a and b . Prompt photon production in hadron collisions is one of the most direct ways to access the gluon structure of hadrons.

Two main hard processes are responsible in the LO for the production of prompt photons in nuclear collisions: i) gluon Compton scattering, $gq(\bar{q}) \rightarrow \gamma q(\bar{q})$, which dominates, and ii)

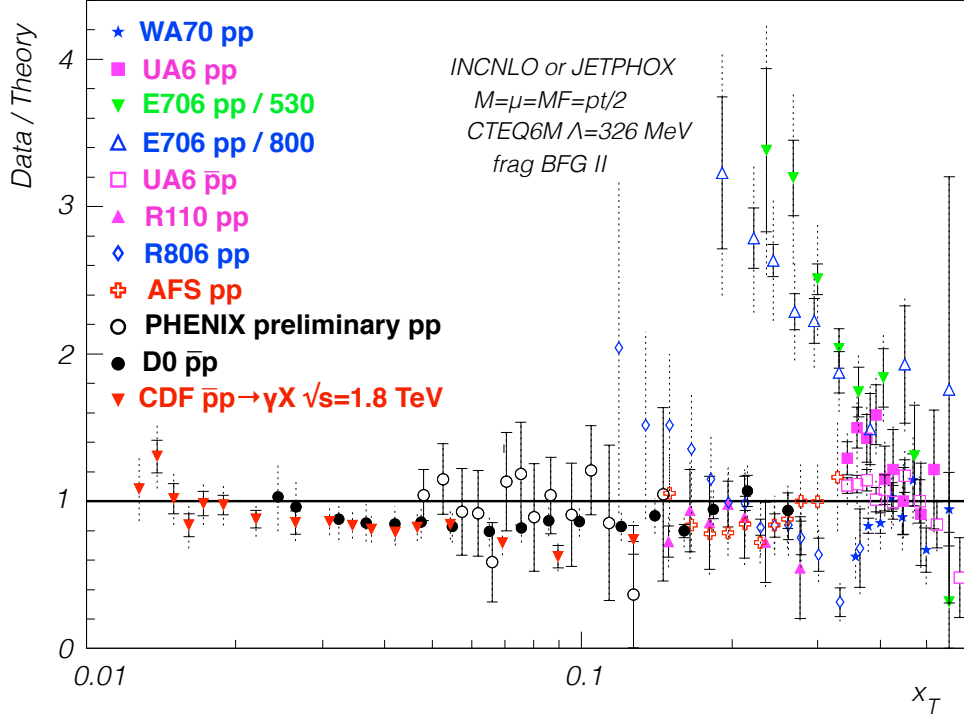


Figure 1. Measured cross sections of prompt-photon production divided to the predicted those by theory as function of x_T [4].

quark-antiquark annihilation, $q\bar{q} \rightarrow \gamma g$. Contribution of the latter process to the total cross section does not exceed 20% at the center-of-mass energy ~ 20 GeV/ c^2 . Hard processes with two prompt photons in the final state, such as $gg \rightarrow \gamma\gamma$ (via a box diagram) and $q\bar{q} \rightarrow \gamma\gamma$ (directly) contribute on a percent level.

Unpolarised measurements of the differential cross section of prompt-photon production in proton-proton(antiproton) collisions were already performed by the fixed-target and collider experiments [3]. Figure 1 shows the ratio of the measured cross sections to the predicted by theory as function of $x_T = 2p_T/\sqrt{s}$ [4] where p_T is the transverse momentum of produced prompt photon. One can see that for fixed-target results corresponding to $\sqrt{s} \sim 20$ GeV, there is a significant disagreement with theoretical expectations that is absent for high-energy collider results. A new precise measurement at low energies could clarify the problem.

The measurement of single transverse spin asymmetry A_N^γ in prompt-photon production at high p_T in polarised p - p and d - d collisions could provide information on the gluon Sivers function, which is almost unknown at the moment [5]. The numerator of A_N^γ can be expressed as [6]

$$\begin{aligned} \sigma^\uparrow - \sigma^\downarrow &= \sum_i \int_{x_{min}}^1 dx_a \int d^2\mathbf{k}_{Ta} d^2\mathbf{k}_{Tb} \frac{x_a x_b}{x_a - (p_T/\sqrt{s}) e^y} [q_i(x_a, \mathbf{k}_{Ta}) \Delta_N G(x_b, \mathbf{k}_{Tb}) \\ &\times \frac{d\hat{\sigma}}{d\hat{t}}(q_i G \rightarrow q_i \gamma) + G(x_a, \mathbf{k}_{Ta}) \Delta_N q_i(x_b, \mathbf{k}_{Tb}) \frac{d\hat{\sigma}}{d\hat{t}}(G q_i \rightarrow q_i \gamma)] . \end{aligned} \quad (2)$$

Here σ^\uparrow and σ^\downarrow are the cross sections of the prompt-photon production for the opposite transverse polarisations of one of the colliding protons, $q_i(x, \mathbf{k}_{Ta})$ [$G(x, \mathbf{k}_{Ta})$] is the quark [gluon] distribution function with specified \mathbf{k}_T and $\Delta_N G(x_b, \mathbf{k}_{Tb})$ [$\Delta_N q_i(x_b, \mathbf{k}_{Tb})$] is the gluon [quark] Sivers function. $d\hat{\sigma}/d\hat{t}$ represents the corresponding gluon Compton scattering cross section. The

authors in [7] pointed out that the asymmetry A_N^γ at large positive x_F is dominated by quark-gluon correlations while at large negative x_F it is dominated by pure gluon-gluon correlations as it was concluded in [8]. The further development of the corresponding formalism can be found in [9, 10]. It is important to notice that the corresponding known non-zero asymmetry in π^0 production, $A_N^{\pi^0}$ [11], could be controlled in parallel.

The first attempt to measure A_N^γ at $\sqrt{s} = 19.4$ GeV was performed in the fixed target experiment E704 at Fermilab in the kinematic range $-0.15 < x_F < 0.15$ and $2.5 \text{ GeV}/c < p_T < 3.1 \text{ GeV}/c$. The results were consistent with zero asymmetry within large statistical and systematic uncertainties [12].

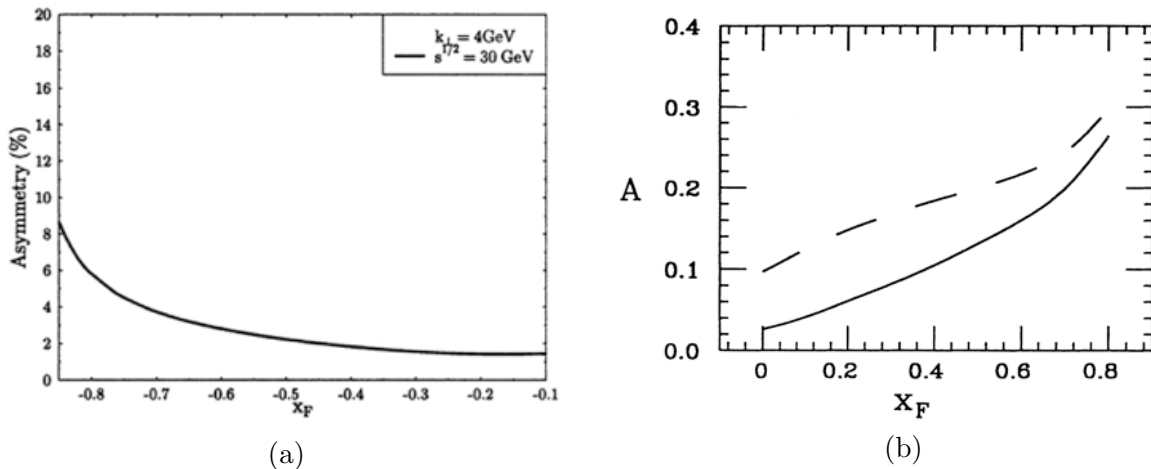


Figure 2. Theoretical predictions for A_N^γ at $\sqrt{s} = 30$ GeV and $p_T = 4$ GeV/c for (a) positive [9] and (b) negative [7] values of x_F .

The study of prompt-photon production at large transverse momentum with longitudinally polarised proton beams could provide the access to gluon polarisation Δg via the measurement of longitudinal double spin asymmetry A_{LL}^γ [13]. Assuming dominance of the gluon Compton scattering process, the asymmetry A_{LL}^γ can be presented as [14]

$$A_{LL} \approx \frac{\Delta g(x_a)}{g(x_a)} \cdot \left[\frac{\sum_q e_q^2 [\Delta q(x_b) + \Delta \bar{q}(x_b)]}{\sum_q e_q^2 [q(x_b) + \bar{q}(x_b)]} \right] \cdot \hat{a}_{LL}(gq \rightarrow \gamma q) + (a \leftrightarrow b). \quad (3)$$

The second factor in the equation coincides to the lowest order with the spin asymmetry A_1^p well-known from polarised DIS, and the partonic asymmetry \hat{a}_{LL} is calculable in the perturbative QCD. Previous results for gluon polarisation show that gluon polarisation is consistent with zero: $|\Delta g/g| < \pm 0.2$ while the asymmetry A_1^p is about 0.2. So it seems that the value of A_{LL}^γ should not exceed the level of a few percent. Measurement of A_{LL}^γ asymmetry as well as A_N^γ is a part of the spin physics programme at the RHIC collider [15, 16, 17, 18, 14].

Authors in [19, 20] propose also to pay attention to associative prompt-photon production in reactions like $pp \rightarrow \gamma J/\psi X$.

3. Prompt photons at SPD

The SPD setup is planned as a universal 4π detector. It consists of three parts: barrel and two end-caps. Each part has an individual magnetic system. The toroidal field should provide tracking capability in the barrel part while the end-caps are equipped by solenoidal coils. Such configuration of the magnetic system should minimize the magnetic field in the beam interaction region. Tracking system (TS) of the SPD setup consists of the silicon-based inner tracker (IT) in

the central part of the detector surrounded by the main tracker using gas-filled drift straw-tubes as the basic detection element. The time-of-flight system (TOF) should provide identification of secondary hadrons in a wide kinematic range. The shashlyk-type electromagnetic calorimeter (ECAL) is responsible for photon reconstruction. It will be the main element for the described programme with prompt photons. The range (muon) system (RS) should perform the advanced muon identification via muonic pattern recognition and further matching of track segments to tracks in the inner part of the detector.

The gluon Compton scattering (GCS) is the main mechanism of the prompt-photon production at SPD energies. At $\sqrt{s} = 26$ GeV, the corresponding cross section calculated for $p_T > 1$ GeV/ c in the leading order is $1.2 \mu\text{b}$. The contribution of the competitive quark-antiquark annihilation process is one order of magnitude smaller. Nevertheless the main source of photons in hadronic collisions is the decay of secondary particles, mainly 2γ decay of π^0 and η mesons. Contributions of photons from decays of different secondary particles per one interaction are presented in Tab. 1. The p_T spectra of the GCS photons and the decay photons produced near the interaction point are shown in Fig. 3(a). The contribution of the decay photons dominates over the GCS signal in full range of p_T but relative fraction of signal photons increases with increasing p_T . The rejection of photons from reconstructed 2γ decays of π^0 and η -mesons and the following Monte Carlo-based statistical subtraction of residual background photons is the only a way to access the prompt-photon production cross section at high p_T .

Table 1. Contributions of photons from decays of different secondary particles per one inelastic interaction (according to Pythia6).

Decay	Number of photons
π^0	8.70
η	0.40
ω	0.06
η'	0.05
Σ^0	0.04
Others	0.01

Other important sources of background clusters in the electromagnetic calorimeter are:

- clusters produced in the interaction of secondary particles with the material of the setup elements;
- "charged" clusters misidentified as neutral in the ECAL due to inefficiency of track finding and reconstruction algorithms;
- overlapping of clusters produced by different particles;
- clusters produced by neutral hadrons.

For successful implementation of the prompt-photon programme the SPD setup and the ECAL have to meet the following requirements:

- inner space of the SPD setup should contain as minimal amount of material as possible in order to keep high transparency of the setup for photons;
- minimal tracking capability should be provided in order to distinguish charged and neutral clusters in ECAL;
- reasonable granularity of the ECAL in order to avoid the pile-up effect that reduces the photon reconstruction efficiency and distorts kinematics of reconstructed photons;

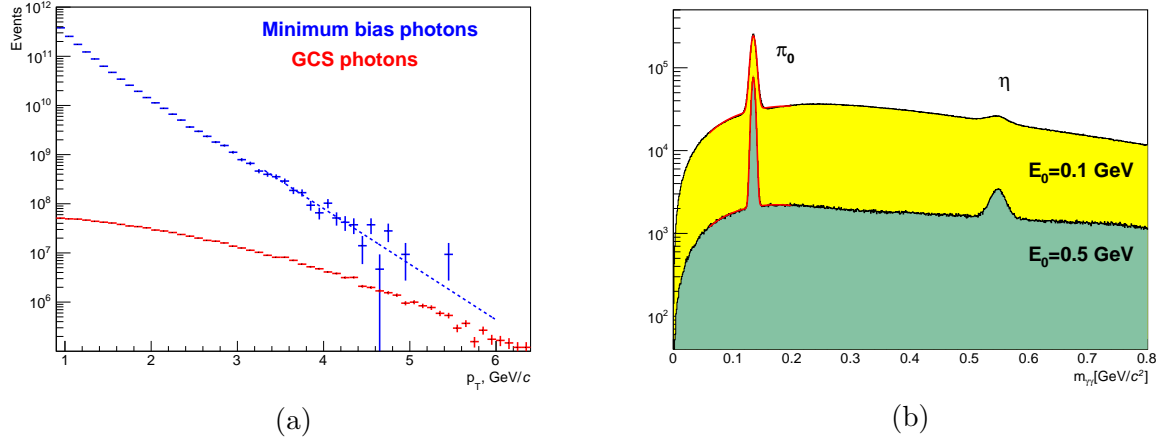


Figure 3. (a) The p_T spectra of GCS prompt photons (red) and photons produced from π^0 decay (blue). (b) The invariant mass spectrum of two photons for two ECAL thresholds: 100 MeV (yellow) and 500 MeV (green).

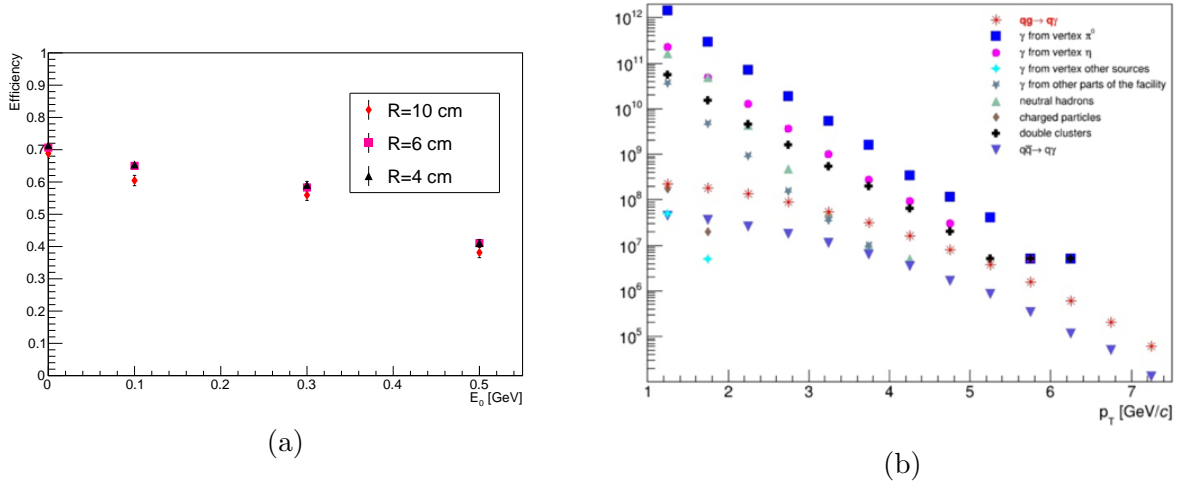


Figure 4. (a) The efficiency of the $\pi^0 \rightarrow \gamma\gamma$ decay reconstruction in case when at least one photon has $p_T > 2$ GeV/c as a function of cluster energy threshold for different granularities R of the ECAL. (b)

- the ability to detect with reasonable resolution an energy deposit down to 100 MeV to keep high reconstruction efficiency for π^0 decays. It is important to note that this threshold is significantly below the MIP signal (~ 200 MeV) for the planned calorimeter.

The invariant mass spectrum of two photons reconstructed in the ECAL with 100 MeV and 200 MeV energy threshold is shown in Fig. 3(b). Relative energy resolution of the ECAL was assumed to be $\sigma_E/E = 1.96\% \oplus 2.74\%/\sqrt{E/GeV}$. Gaussian width of the π^0 peak is 4.6 MeV/ c^2 and 3.15 MeV/ c^2 for 100 MeV and 500 MeV thresholds, respectively. Figure 4(a) shows the efficiency of the $\pi^0 \rightarrow \gamma\gamma$ decay reconstruction for different cluster energy thresholds and different granularities of the ECAL. More kinematic distributions could be found at [21]. Contributions of the signal and each kind of background mentioned above are shown in Fig. 4(b). Tracking efficiency is assumed to be on the level of 90% while the ECAL cell size is 4 cm [22].

The accuracy of the prompt-photon production cross section and asymmetries A_N and A_{LL} in

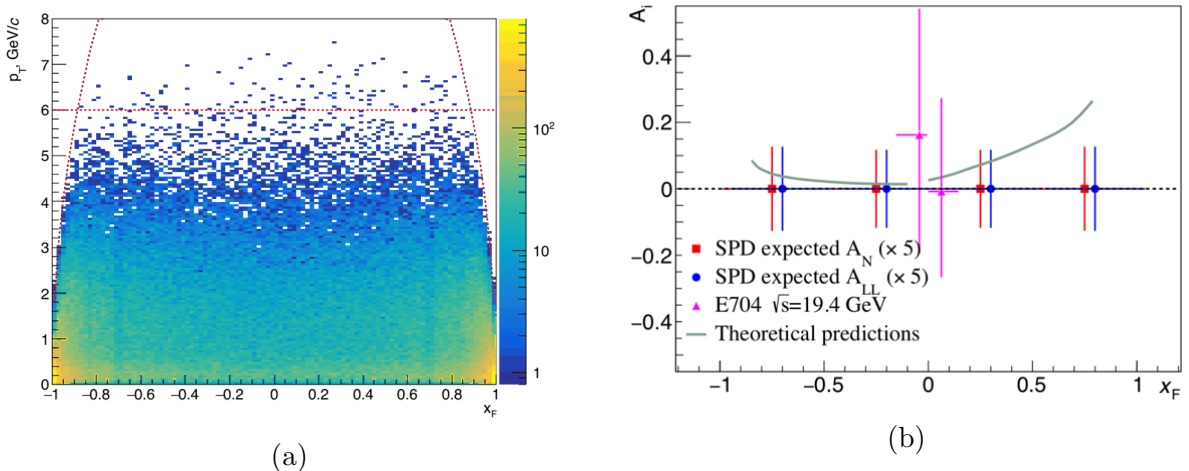


Figure 5. (a) p_T distribution for GCS photons vs. x_F . (b) Expected accuracy of A_N and A_{LL} measurement as a function of x_F .

p - p collisions is estimated on the basis of the following assumptions. Data sample corresponds to 10^7 s of data taking (about 100 days) with average luminosity $L = 10^{32} \text{ s}^{-1} \text{ cm}^{-2}$. The inefficiency of the photon reconstruction is caused only by geometrical acceptance and material distribution, no threshold for photon reconstruction in the ECAL. LO calculations are used for the GCS cross-section. Only $\pi^0 \rightarrow \gamma\gamma$ decay is taken into account as background. Average π^0 reconstruction efficiency is about 70%. Relative accuracy for the Monte Carlo description of photon reconstruction is assumed to be 2%. Two subsamples with equal statistics are collected with each combination of spin orientations. Absolute polarisation of the beam is assumed to be exactly equal to 100%. We also ignore any uncertainties related with the control of the beam polarisation(s) and luminosity.

Since low- p_T region is useless due to a huge background while at high- p_T the statistics is very limited, a reasonable cut on transverse momentum of photon has to be applied in order to maximize the accuracy of the planned measurements. For the running conditions mentioned above the optimal value lies in the range from 5 to 6 GeV/ c . The total amount of the detected GCS photons with $p_T > 5$ GeV/ c is expected to be about 6×10^6 .

Figure 5(a) shows the distribution of p_T vs. x_F for GCS photons. The expected accuracy of A_N and A_{LL} measurement in each of four intervals in x_F in the range from -0.89 to 0.89 is shown in Fig 5(b). The results of previous measurement and the theoretical expectations are also presented on the plot.

4. Summary

Unpolarised and polarised physics with prompt photons looks very attractive since all previous the measurements at energy scale of about 20 GeV were performed 20–30 years ago. It is a good time to come back with a new level of experimental techniques and theoretical understanding. The SPD detector at the NICA collider provides a good chance to perform such kind of measurements. Preliminary analysis of the background conditions shows that the measurement of asymmetries in the prompt-photon production cross section on the level of a few per cent is possible at SPD conditions. Taking into account quite minimalistic requirements to the tracking system of the SPD detector, the study of the prompt-photon production could be the first stage of the SPD setup operation.

References

- [1] Savin I, Efremov A, Peshekhonov D, Kovalenko A, Teryaev O, Shevchenko O, Nagajcev A, Guskov A, Kukhtin A and Topilin N 2015 *EPJ Web of Conferences* **85** 02039
- [2] SPD working group 2018 *Conceptual design of the Spin Physics Detector*
- [3] Vogelsang W and Whalley M R 1997 *J. Phys. G* **23** A1
- [4] Aurenche P, Fontannaz M, Guillet G P, Pilon E and Werlen M 2006 *Phys. Rev. D* **73** 094007
- [5] Boer D, Lorc C, Pisano C and Zhou J 2015 *Adv. High Energy Phys.* **2015**, 371396
- [6] Schmidt I, Soffer J and Yang J J 2005 *Phys. Lett. B* **612** 258
- [7] Qiu J W and Sterman G F 1992 *Nucl. Phys. B* **378** 52
- [8] Ji X D 1992 *Phys. Lett. B* **289** 137
- [9] Hammon N, Ehrnsperger B and Schaefer A 1998 *J. Phys. G* **24** 991
- [10] Gamberg L and Kang Z B 2012 *Phys. Lett. B* **718** 181
- [11] Adams D L *et al.* [E581 and E704 Collaborations] 1991 *Phys. Lett. B* **261** (1991) 201
- [12] Adams L G *et al.* [E704 Collaboration] 1995 *Phys. Lett. B* **345** 569
- [13] Cheng H Y and Lai S N 1990 *Phys. Rev. D* **41** 91
- [14] Bunce G, Saito N, Soffer J and Vogelsang W 2000 *Ann. Rev. Nucl. Part. Sci.* **50** 525
- [15] Jalilian-Marian J, Orginos K and Sarcevic I 2001 *Phys. Rev. C* **63** 041901
- [16] Sakashita K 2009 *Cross Section for Prompt Photon Production in Proton-Proton Collisions at $\sqrt{s} = 62.4$ GeV* PhD thesis
- [17] Horaguchi T 2006 *Prompt photon production in proton proton collisions at $\sqrt{s} = 200$ GeV* PhD thesis
- [18] Skoro G P, Zupan M and Tokarev M V 1999 *Nuovo Cim. A* **112** 809
- [19] Li R and Wang J X 2009 *Phys. Lett. B* **672** 51
- [20] Lansberg J P 2016 *Int. J. Mod. Phys. Conf. Ser.* **40** 1660015
- [21] Guskov A 2014 *Proc. XV Advanced Research Workshop on High Energy Spin Physics (DSPIN-13)* p 363
- [22] Rymbekova A 2019 *Ukr. J. Phys.* **64** 631